

The fine structure of microwave-induced magneto-oscillations in photoconductivity of the two-dimensional electron system formed on a liquid-helium surface

Yu.P. Monarkha¹

¹*Institute for Low Temperature Physics and Engineering, 47 Lenin Avenue, 61103 Kharkov, Ukraine*

The influence of the inelastic nature of electron scattering by surface excitations of liquid helium (ripples) on the shape of magnetoconductivity oscillations induced by resonance microwave (MW) excitation is theoretically studied. The MW field provides a substantial filling of the first excited surface subband which sparks off inter-subband electron scattering by ripples. This scattering is the origin of magneto-oscillations in the momentum relaxation rate. The inelastic effect becomes important when the energy of a ripplon involved compares with the collision broadening of Landau levels. Usually, such a condition is realized only at sufficiently high magnetic fields. On the contrary, the inelastic nature of inter-subband scattering is shown to be more important in a lower magnetic field range because of the new enhancement factor: the ratio of the inter-subband transition frequency to the cyclotron frequency. This inelastic effect affects strongly the shape of conductivity oscillations which acquires an additional wavy feature (a mixture of splitting and inversion) in the vicinity of the level-matching points where the above noted ratio is close to an integer.

PACS numbers: 73.40.-c, 73.20.-r, 73.25.+i, 78.70.Gq

I. INTRODUCTION

Microwave-induced magnetoconductivity oscillations, whose minima evolve into novel zero-resistance states at high microwave (MW) power, were first observed in degenerate semiconductor two-dimensional (2D) electron systems¹⁻³. In these experiments, the magnetic field \mathbf{B} was directed normally to the electron layer, and the MW frequency ω was substantially larger than the cyclotron frequency $\omega_c = eB/mc$. These observations have attracted much theoretical interest and sparked invention of a wide variety of theoretical mechanisms⁴⁻⁶ intended to explain remarkable $1/B$ -periodic oscillations and the appearance of zero-resistance states.

Recently, similar $1/B$ -periodic magnetoconductivity oscillations were observed in a particularly simple nondegenerate multi-subband 2D electron liquid formed on the free surface of liquid ^3He ^{7,8}. Their minima also evolve into zero-resistance states at high MW power. Still, there is an important difference between results reported for surface electrons (SEs) in liquid helium and those obtained for semiconductor systems. In experiments¹⁻³, ω is quite arbitrary: $\omega > \omega_c$. To observe magneto-oscillations in the electron system formed on the liquid-helium surface it is necessary that the MW frequency ω be equal to the resonance frequency $\omega_{2,1} = (\Delta_2 - \Delta_1)/\hbar$ for electron excitation to the next surface subband. The sequence Δ_l (here $l = 1, 2, \dots$) describes the energy spectrum of electron subbands formed at the free surface of liquid helium because of the interplay of the attractive image force and the potential barrier $V_0 \sim 1$ eV at the interface^{9,10}. In the limit of low holding electric fields E_\perp directed normally to the interface, $\Delta_{2,1} \equiv \Delta_2 - \Delta_1 \simeq 3.2$ K for liquid ^3He and $\Delta_{2,1} \simeq 5.7$ K for liquid ^4He . Thus, in experiments on semiconductor systems, higher electron subbands were not excited by the MW field, whereas in experiments with SEs^{7,8} there is a substantial

fraction of electrons occupied the first excited subband because of the MW resonance.

The theory explaining MW-resonance-induced magnetoconductivity oscillations observed for SEs on liquid helium was worked out^{11,12} using the quasi-elastic approximation for electron scattering by ripples and vapor atoms. This approximation assumes that the energy exchange at a collision is much smaller than the collision broadening of Landau levels.

The origin of magneto-oscillations and negative conductivity effects induced by resonance MW excitation can be seen already from a simple analysis of the energy conservation for usual inter-subband electron scattering (not involving photons) in the presence of the uniform driving electric field E_\parallel . According to this analysis, for the electron spectrum

$$\varepsilon_{l,n,X} = \Delta_l + \hbar\omega_c (n + 1/2) + eE_\parallel X \quad (1)$$

(here X is the center coordinate of the cyclotron orbit), the decay of an excited subband $l \rightarrow l'$ ($l > l'$, $\Delta_{l,l'} = \Delta_l - \Delta_{l'} > 0$, and $n' - n = m^* > 0$) results in displacements of the orbit center

$$X' - X = \frac{\hbar\omega_c}{eE_\parallel} \left(\frac{\Delta_{l,l'}}{\hbar\omega_c} - m^* \right) \quad (2)$$

proportional to the quantity $(\Delta_{l,l'}/\hbar\omega_c - m^*)$. This quantity changes its sign at the level-matching points B_{m^*} defined by the condition $\Delta_{l,l'}/\hbar\omega_c = m^*$ (here m^* is an integer). At $B < B_{m^*}$, the displacement $X' - X > 0$ and, therefore, the decay of the excited subband is accompanied by electron scattering against the driving force.

Somehow, Eq. (2) resembles the displacement mechanism of the negative conductivity effect discussed broadly for semiconductor systems¹³ where in a similar equation the photon quantum $\hbar\omega$ stands instead of $\Delta_{l,l'}$. In that theory, the sign-changing correction to σ_{xx} is due to radiation-induced disorder-assisted current, and the

photon energy enters the energy conservation law. The important point is that here photons are not involved in inter-subband scattering directly and the condition $X' - X > 0$ found for decay processes is not sufficient for obtaining negative corrections to the momentum relaxation rate. Naturally, a reverse electron scattering from the ground subband to the excited subband results in $X' - X < 0$, and the negative conductivity effect is fully compensated if the electron system is in equilibrium, and fractional occupancies of surface subbands obey the condition $\bar{n}_l \equiv N_l/N_e = e^{-\Delta_{l,l'}/T_e} \bar{n}_{l'}$ (here T_e is the electron temperature).

The important role of the resonant MW field is to provide an extra filling of the excited subband to break the balance of inter-subband scattering mentioned above. For example, the decay of the first excited subband ($l = 2$) to the ground subband ($l = 1$) caused by quasi-elastic scattering is possible only if B is close to the level-matching points B_{m^*} , because $|X' - X|$ is restricted by the magnetic length. If B is substantially away from these level-matching points, the quasi-elastic decay is impossible and $\bar{n}_2 \simeq \bar{n}_1 \simeq 1/2$ because of MW excitation. Under a weak driving field, the width of regions of the magnetic field near B_{m^*} , where the excited subband decays quasi-elastically, is determined by the collision broadening of the corresponding Landau levels. Within these regions, the momentum relaxation rate of SEs caused by inter-subband scattering^{11,12}

$$\nu_{\text{inter}} \propto - \left(\frac{\omega_{2,1}}{\omega_c} - m^* \right) (\bar{n}_2 - e^{-\Delta_{2,1}/T_e} \bar{n}_1). \quad (3)$$

Therefore, the condition $\bar{n}_2 > e^{-\Delta_{2,1}/T_e} \bar{n}_1$ is crucial for the appearance of negative corrections to the momentum relaxation rate ν and to magnetoconductivity σ_{xx} . An increase in \bar{n}_2 caused by trivial heating of SEs obviously cannot lead to the sign-changing term.

The above noted analysis assumes that the ripplon energy $\hbar\omega_q$ can be neglected as compares to typical electron energies. In the absence of the magnetic field, this is the conventional approximation because $\hbar\omega_q \ll T$ for ripplons involved in scattering events. Under a magnetic field applied perpendicular to the electron layer, there is an additional energy parameter which describes the width of the single-electron density of states: the collision broadening of Landau levels Γ_n . For SEs on liquid helium, Landau levels are extremely narrow: $\Gamma_n \ll T$. Wave vectors of ripplons involved in electron scattering $q \sim 1/L_B$ [here $L_B = \sqrt{\hbar c/eB}$ is the magnetic length], and the energy exchange $\hbar\omega_q \propto q^{3/2}$ increases with B faster than Γ_n which is approximately proportional to \sqrt{B} . Therefore, in a high magnetic field range, depending on temperature ($\Gamma_n \propto \sqrt{T}$), $\hbar\omega_q$ becomes comparable with Γ_n , and electron scattering is suppressed.

Experimental observation^{14,15} indicates that the inelastic effect on the quantum magnetotransport becomes substantial at $T \sim 0.1 - 0.2$ K and $B > 1$ T, and the suppression of σ_{xx} is the stronger the higher magnetic field is applied. Simple estimates allow to assume that

similar conditions can be realized in an experiment on magneto-oscillations in photoconductivity of SEs on liquid ⁴He, because the corresponding excitation frequency $\omega_{2,1}$ is high, and the level-matching points $B_{m^*} > 1$ T, if $m^* < 4$. In this case, the inelastic effect can cause additional variations of the shape of magnetoconductivity oscillations in the vicinity of the level-matching points B_{m^*} , which could be used for experimental identification of the microscopic mechanism of zero-resistance states and the resonant photovoltaic effect discovered recently¹⁶.

In this work, we report the theory of magnetoconductivity oscillations induced by resonance MW excitation which takes into account the inelastic nature of the decay of excited subbands caused by electron-ripplon interaction. We show that for inter-subband scattering the inelastic effect displays differently as compared to the equilibrium magnetotransport in a single subband. In our treatment, the maximum of the decay rate of an excited subband is naturally split near the level-matching points B_{m^*} because of one-ripplon creation and destruction processes. The unusual thing is that this inelastic effect increases with m^* , and therefore extends itself into the lower magnetic field range $B < 1$ T.

We show also that the inelastic effect on the momentum relaxation rate of the electron layer caused by inter-subband scattering cannot be reduced to simple splitting similar to that of the decay rate. In magnetoconductivity curves, this effect displays itself as a combination of splitting and inversion. As a result, σ_{xx} develops a new remarkable wavy feature in the vicinity of the level-matching points. The influence of both mutual electron interaction and electron heating on the new fine structure of MW-induced magneto-oscillations is also analyzed.

II. INELASTIC INTER-SUBBAND SCATTERING AND MOMENTUM RELAXATION

The most interesting features of MW-induced magnetoconductivity oscillations such as zero-resistance states are observed^{7,8} in the low temperature range ($T \sim 0.2$ K) where SEs are predominantly scattered by capillary wave quanta (ripplons). Ripplons represent a sort of 2D phonons with an unusual spectrum $\omega_q = \sqrt{\alpha/\rho} q^{3/2}$, where α and ρ are the surface tension and mass density of liquid helium, correspondingly. Therefore, the Hamiltonian of electron-ripplon interaction is similar to the Hamiltonian of electron-phonon interaction in solids

$$H_{\text{int}}^{(e-R)} = \sum_{\epsilon} \sum_{\mathbf{q}} U_q(z_e) Q_q \left(b_{\mathbf{q}} + b_{-\mathbf{q}}^{\dagger} \right) e^{i\mathbf{q}\mathbf{r}_e}, \quad (4)$$

where $b_{\mathbf{q}}$ and $b_{\mathbf{q}}^{\dagger}$ are destruction and creation operators, $Q_q^2 = \hbar q / 2\rho\omega_q$, and $U_q(z_e)$ is the electron-ripplon coupling whose properties and matrix elements $\langle l | U_q(z) | l' \rangle \equiv (U_q)_{l,l'}$ are well defined in the literature^{15,17}.

To describe quantum magnetotransport of a 2D electron gas it is conventional to use the self-consistent Born approximation (SCBA) theory¹⁸ or the linear response theory¹⁹ with the proper approximation for the electron density-of-states function. Unfortunately, these approaches cannot be applied directly to the SE system under resonance MW excitation. In these theories, conductivity is an equilibrium property of the system, whereas here we need to describe conductivity of the system which is far away from its equilibrium state. In our conductivity treatment, we intend also to include strong Coulomb interaction between electrons whose average potential energy can be much higher than the average kinetic energy. For this purposes, it is necessary to use an extension of the SCBA theory applicable for arbitrary subband occupancies \bar{n}_l and $T_e \geq T$.

Firstly, we note that the well-known results of the SCBA theory and Kubo equations for magnetoconductivity of the 2D electron gas can be reproduced in a quite direct way by simple evaluation of the momentum gained by scatterers¹⁵, if scattering probabilities of the Born approximation are taken in the proper form which includes the contribution from high order terms (self-energy effects). This kind of probabilities were actually given already in the Kubo theory¹⁹. Here we express these probabilities through a quite general correlation function of the multi-subband 2D electron system which preserves basic equilibrium properties of the in-plane motion and, at the same time, is independent of subband occupancies.

Consider the average probability of both intra and inter-subband scattering ($l \rightarrow l'$) which is accompanied by the momentum exchange $\hbar\mathbf{q}$ caused by ripplon destruction $\bar{\nu}_{l,l'}^{(-)}(\mathbf{q})$ and creation $\bar{\nu}_{l,l'}^{(+)}(\mathbf{q})$. Conventional Born approximation yields

$$\bar{\nu}_{l,l'}^{(-)}(\mathbf{q}) = \frac{2\pi\hbar}{A} u_{l,l'}^2 \langle \sum_{n',X'} \left| (e^{i\mathbf{q}\mathbf{r}_e})_{l,X;l',X'} \right|^2 \times \\ \times \delta(\varepsilon_n - \varepsilon_{n'} + \Delta_{l,l'} + \hbar\omega_q + eE_{\parallel}X - eE_{\parallel}X') \rangle_{\text{in}}, \quad (5)$$

where ε_n represents Landau levels, $\langle \dots \rangle_{\text{in}}$ means averaging over initial in-plane states for the given surface subband l , and we have introduced

$$u_{l,l'}^2(x_q) = \frac{A}{\hbar^2} N_q Q_q^2 \left| (U_q)_{l,l'} \right|^2 \simeq \frac{TL_B^2}{4\alpha\hbar^2 x_q} \left| (U_q)_{l,l'} \right|^2 \quad (6)$$

as the function of the dimensionless parameter $x_q = q^2 L_B^2 / 2$. For $q \lesssim 1/L_B$, the distribution function of ripples $N_q \simeq T/\hbar\omega_q$. In the following, the surface area A will be set to unity. It is well known that $\left| (e^{i\mathbf{q}\mathbf{r}_e})_{l,X;l',X'} \right|^2$ can be written as $J_{n,n'}^2(q) \delta_{X',X-q_y l_B^2}$, where $J_{n,n'}^2(q)$ is a function of the absolute value of the 2D wave-vector. The exact expression for $J_{n,n'}^2(q)$ is given in the literature (for recent examples, see^{17,20}).

According the relationship $X' - X = -q_y L_B^2$ the quantity to be averaged in Eq. (5) does not depend on X ,

and, therefore, Eq. (5) actually contains the averaging over discrete Landau numbers n only. It is natural to assume that a weak dc driving field E_{\parallel} does not change electron distribution over Landau levels, and one can use the distribution function $e^{-\varepsilon_n/T_e}/Z_{\parallel}$ for the averaging operation. This is quite clear in the absence of scatterers, because under the magnetic field a driving electric field can be eliminated by a proper choice of the inertial reference frame: $\mathbf{E}' = \mathbf{E} - \mathbf{B} \times \mathbf{V}/c \rightarrow 0$. Moreover, if there is no a driving electric field in the laboratory frame, it appears in any other inertial reference frame. At a low drift velocity of the electron system, quasi-elastic scattering cannot change the population of Landau levels. The above given statement is also verified by the comparison of the results obtained in the treatment considered here with the well-known results of the conventional SCBA at zero MW power.

Following the procedure described in the linear response theory¹⁹, and taking into account that $l_B^2 e E_{\parallel} = \hbar V_H$ (here $V_H = cE_{\parallel}/B$ is the absolute value of the Hall velocity), Eq. (5) can be transformed into the form containing level densities of the initial and final states

$$\bar{\nu}_{l,l'}^{(-)}(\mathbf{q}) = u_{l,l'}^2 S_{l,l'}(q, \omega_{l,l'} + \omega_q + q_y V_H), \quad (7)$$

where

$$S_{l,l'}(q, \Omega) = \frac{2}{\pi\hbar Z_{\parallel}} \sum_{n,n'} J_{n,n'}^2(q) \times \\ \times \int d\varepsilon e^{-\varepsilon/T_e} \text{Im} G_{l,n}(\varepsilon) \text{Im} G_{l',n'}(\varepsilon + \hbar\Omega). \quad (8)$$

Here $G_{l,n}(\varepsilon)$ is the single-electron Green's function of the corresponding subband whose imaginary part is a substitute of $-\pi\hbar\delta(\varepsilon - \varepsilon_n)$. We retain the index l keeping in mind further broadening due to interaction with scatterers because its strength is different for different surface subbands. Similar equation can be found for ripplon creation processes:

$$\bar{\nu}_{l,l'}^{(+)}(\mathbf{q}) = e^{\hbar\omega_q/T} u_{l,l'}^2 S_{l,l'}(q, \omega_{l,l'} - \omega_q + q_y V_H). \quad (9)$$

At $l = l'$ the function $S_{l,l'}(q, \Omega)$ coincides with the dynamic structure factor (DSF) of a nondegenerate 2D electron gas. It should be noted that the above given equations resemble scattering cross-sections of thermal neutrons and X-rays in solids²¹. Here scatterers (ripples) play the role of particle fluxes whereas the electron layer represents a target.

The self-energy effects (high order terms), which are very important for 2D electron systems under a quantizing magnetic field, are taken into account by inclusion of the collision broadening $\Gamma_{l,n}$ of Landau levels of a given surface subband (l) according to the cumulant approach²²:

$$-\text{Im} G_{l,n}(\varepsilon) = \frac{\sqrt{2\pi}\hbar}{\Gamma_{l,n}} \exp \left[-\frac{2(\varepsilon - \varepsilon_n)^2}{\Gamma_{l,n}^2} \right]. \quad (10)$$

Thus, similarly to the Kubo presentation¹⁹, the average probabilities of electron scattering with the momentum exchange $\hbar\mathbf{q}$ are expressed in terms of density-of-state functions of the initial and final states broadened because of interaction with scatterers. For the Gaussian shape of level densities, the integral entering the definition of $S_{l,l'}(q, \Omega)$ can be evaluated analytically¹². Moreover, this kind of a level density represents a good starting point for obtaining an analytical form of $S_{l,l'}(q, \Omega)$ for the multi-subband 2D Coulomb liquid¹⁷.

The Eq. (8) is a useful generalization of the DSF for the multi-subband 2D electron system because it preserves the important property of the equilibrium of the in-plane motion

$$S_{l',l}(q, -\Omega) = e^{-\hbar\Omega/T_e} S_{l,l'}(q, \Omega), \quad (11)$$

and, at the same time, it does not depend on \bar{n}_l , which allows to describe momentum relaxation for arbitrary subband occupancies. The property of Eq. (11) simplifies evaluations of the momentum relaxation rate. For example, using this property average probabilities for the reverse scattering processes discussed in the Introduction can be transformed into the same quantities of the direct processes:

$$\bar{\nu}_{l',l}^{(+)}(\mathbf{q}) = e^{-\Delta_{l,l'}/T_e} e^{\hbar\omega_q(1/T-1/T_e)} e^{\hbar q_y V_H/T_e} \bar{\nu}_{l,l'}^{(-)}(-\mathbf{q}), \quad (12)$$

$$\bar{\nu}_{l',l}^{(-)}(\mathbf{q}) = e^{-\Delta_{l,l'}/T_e} e^{\hbar\omega_q(1/T_e-1/T)} e^{\hbar q_y V_H/T_e} \bar{\nu}_{l,l'}^{(+)}(-\mathbf{q}). \quad (13)$$

We shall use these relationships in the following analysis.

The introduced above quantities $\bar{\nu}_{l,l'}^{(\pm)}(\mathbf{q})$ represent useful assemblies to construct major relaxation rates of the multi-subband 2D electron system under a quantizing magnetic field such as the decay rate of an excited subband and the momentum relaxation rate due to inter-subband scattering. It is important that they preserve peculiarities of quantum magnetotransport in two-dimensions. They include the self-energy effects eliminating magnetoconductivity singularities, the effect of the driving electric field and, after the following generalization, can even include strong Coulomb forces acting between electrons.

A. The many-electron effect

Even for the lowest electron areal density n_e (about $1 \times 10^6 \text{ cm}^{-2}$) used in the experiments on SEs in liquid helium^{7,8}, Coulomb interaction between SEs cannot be neglected. For example, at $T \simeq 0.2 \text{ K}$ the average interaction energy per an electron U_C is much larger than the average kinetic energy (T). The generalized DSF of the multi-subband 2D electron system applicable for such conditions was found in Ref. 17:

$$S_{l,l'}(\Omega) = \frac{2\sqrt{\pi}\hbar}{Z_{\parallel}} \sum_{n,n'} \frac{J_{n,n'}^2}{\bar{\Gamma}_{l,n;l',n'}} \exp\left[-\frac{\varepsilon_n}{T_e} - D_{l,n;l',n'}(\Omega)\right], \quad (14)$$

where

$$D_{l,n;l',n'} = \frac{\hbar^2 \left(\Omega - m^* \omega_c - \frac{\Gamma_{l,n}^2 + x_q \Gamma_C^2}{4T_e \hbar} \right)^2}{\bar{\Gamma}_{l,n;l',n'}} - \frac{\Gamma_{l,n}^2}{8T_e^2}, \quad (15)$$

$$\bar{\Gamma}_{l,n;l',n'}^2(x_q) = \frac{\Gamma_{l,n}^2 + \Gamma_{l',n'}^2}{2} + x_q \Gamma_C^2, \quad (16)$$

$m^* = n' - n$, $\Gamma_C = \sqrt{2}eE_f^{(0)}L_B$ and $E_f^{(0)} \simeq 3\sqrt{T_e n_e^{3/4}}$. The quantity $E_f^{(0)}$ represents the typical quasi-uniform electric field of other electrons acting on a given electron because of thermal fluctuations²³. Here and in some following equations we do not show explicitly the dependence on q of functions $S_{l,l'}$, $J_{n,n'}^2$, etc., in order to shorten lengthy equations. In the limiting case $\Gamma_C \rightarrow 0$, Eq. (14) transforms into the generalized DSF of the multi-subband 2D system of noninteracting electrons.

The function $S_{l,l'}(\Omega)$ has sharp maxima when $\hbar\Omega$ is close to Landau excitation energies $(n' - n)\hbar\omega_c$. These maxima are broadened because of electron interaction with scatterers and because of the fluctuational electric field \mathbf{E}_f . It is important that Coulomb broadening of the DSF $\sqrt{x_q}\Gamma_C$ is not equivalent to the collision broadening because it depends on q through the dimensionless parameter $x_q = q^2 L_B^2/2$. The fluctuational field does not broaden the single-electron level densities, because, as noted above, it can be eliminated by a proper choice of the inertial reference frame moving along the layer¹⁵.

Small frequency shifts in the general expression for $S_{l,l'}(\Omega)$ play very important role: they provide the basic property of Eq. (11). The small shift $\Gamma_{l,n}^2/4T_e\hbar$ can be neglected only for substantially positive values of Ω . Therefore, it is convenient to transform terms containing $S_{l,l'}(\Omega)$ with negative Ω into forms with positive Ω employing the relationship of Eq. (11). It worth noting also that the Coulomb shift in the frequency argument of the DSF $x_q\Gamma_C^2/4T_e\hbar$ increases with x_q and $E_f^{(0)}$ faster than the Coulomb broadening $\sqrt{x_q}\Gamma_C$ which curiously affects positions of magnetoconductivity extremes¹⁷. Therefore, we shall retain it in $S_{l,l'}(\Omega)$ even for substantially positive values of the frequency argument.

B. The decay rate of an excited subband

The decay rate of an excited subband l due to electron scattering down to a lower subband $l' < l$ is easily expressed in terms of $\bar{\nu}_{l,l'}^{(-)}(\mathbf{q})$ and $\bar{\nu}_{l,l'}^{(+)}(\mathbf{q})$:

$$\bar{\nu}_{l \rightarrow l'} = \sum_{\mathbf{q}} \left[\bar{\nu}_{l,l'}^{(+)}(\mathbf{q}) + \bar{\nu}_{l,l'}^{(-)}(\mathbf{q}) \right]. \quad (17)$$

Here, we can neglect the small corrections $q_y V_H$ in the frequency argument of the generalized DSF entering Eqs. (7) and (9). Then, using Eqs. (12) and (13), one

can see that for inelastic scattering the detailed balancing $\bar{\nu}_{l' \rightarrow l} = e^{-\Delta_{l,l'}/T_e} \bar{\nu}_{l \rightarrow l'}$ is fulfilled only if the electron temperature coincides with the temperature of the environment. Anyway, because of the condition $\hbar\omega_q \ll T$ discussed above, the detailed balancing is approximately valid even at high electron temperatures.

When evaluating $\bar{\nu}_{l \rightarrow l'}$ in the ultra-quantum limit $\hbar\omega_c \gg T_e$ ($n = 0$) one can use the approximate expression for the generalized DSF,

$$S_{l,l'}(q, \omega_{l,l'} \pm \omega_q) \simeq 2\sqrt{\pi}\hbar \sum_{m=0}^{\infty} \frac{x_q^m e^{-x_q}}{m! \tilde{\Gamma}_{l,0;l',m}} I_{l,l';m}^{(\pm)}(x_q), \quad (18)$$

applicable for positive values of the frequency argument. Here we introduce functions

$$I_{l,l';m}^{(\pm)}(x_q) = \exp \left\{ - \left[R_{l,l';m}^{(\pm)}(x_q) \right]^2 \right\}, \quad (19)$$

and

$$R_{l,l';m}^{(\pm)}(x_q) = \frac{(\hbar\omega_{l,l'} \pm \hbar\omega_q - m\hbar\omega_c - x_q\Gamma_C^2/4T_e)}{\tilde{\Gamma}_{l,0;l',m}}, \quad (20)$$

It should be noted that in Eqs. (19) and (20) we have omitted small frequency shifts of the order $\Gamma_{l,0}/4T_e$, because the frequency argument of $S_{l,l'}$ in Eq. (18) is substantially positive for decay processes.

Employing the above given notations $\bar{\nu}_{l \rightarrow l'}$ can be transformed into

$$\begin{aligned} \bar{\nu}_{l \rightarrow l'} &= \frac{T}{4\sqrt{\pi}\alpha\hbar} \sum_{m=1}^{\infty} \frac{1}{m!} \int_0^{\infty} \frac{|(U_q)_{l,l'}|^2}{\tilde{\Gamma}_{l,0;l',m}} x_q^{m-1} e^{-x_q} \times \\ &\times \left[I_{l,l';m}^{(-)}(x_q) + I_{l,l';m}^{(+)}(x_q) \right] dx_q. \end{aligned} \quad (21)$$

From this equation it is quite clear that the inelastic effect splits the decay maximum of the elastic theory into two maxima when $\hbar\omega_q = \hbar\sqrt{\alpha/\rho}2^{3/4}x_q^{3/4}/L_B^{3/2}$ becomes comparable with the broadening $\tilde{\Gamma}_{l,0;l',m}$. It is very important that the position of the maximum of the function $x_q^{m-1}e^{-x_q}$ entering the integrand of Eq. (21) (x_q)_{max} increases strongly with the level-matching number m , whereas $\tilde{\Gamma}_{l,0;l',m}$ is nearly independent of m if electron density is sufficiently low. This leads to unexpected enhancement of the inelastic effect in the low magnetic field range where $m^* = \text{round}(\omega_{2,1}/\omega_c)$ is larger.

The above stated is illustrated in Fig. 1 where $\bar{\nu}_{2 \rightarrow 1}$ is shown as the function of $\omega_{2,1}/\omega_c(B) - m^*$ for $m^* = 1, 2, \dots, 7$. Conditions of the figure are chosen to be such ($n_e = 1 \times 10^6 \text{ cm}^{-2}$ and $T = 0.2 \text{ K}$) that the splitting of the decay maximum is absent at $m^* = 1$ ($B \rightarrow B_1$), however, it appears near some lower level-matching points B_{m^*} . At the lowest B_{m^*} ($m^* = 7$), the splitting disappears again because of the Coulombic correction $x_q\Gamma_C^2$ to $\tilde{\Gamma}_{l,0;l',m}^2$ which also increases strongly with m^* .

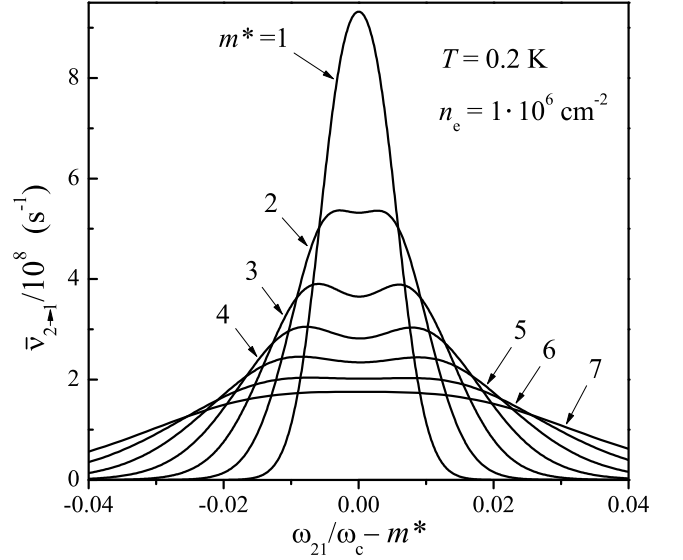


FIG. 1. The decay rate of the first excited subband $\bar{\nu}_{2 \rightarrow 1}$ vs $\omega_{2,1}/\omega_c(B) - m^*$ for different level-matching numbers m^* .

C. Subband occupancies

Under the condition of the MW resonance $\omega = \omega_{2,1}$, the stimulated photon absorption (emission) rate $r_{mw} = \Omega_R^2/2\gamma_{mw}$, where γ_{mw} is the half-width of the resonance, and $\Omega_R = e \langle z | 1 \rangle E_{mw}/\hbar$ is the Rabi frequency proportional to the amplitude of the MW field E_{mw} . In dynamic equilibrium, the fractional occupancies \bar{n}_l are found from the time-independent rate equation. In the framework of the two-subband model ($\bar{n}_1 + \bar{n}_2 = 1$), the solution of the rate equation for the relative occupancy has the following form²⁴

$$\frac{\bar{n}_2}{\bar{n}_1} = \frac{r_{mw} + e^{-\Delta_{2,1}/T_e} \bar{\nu}_{2 \rightarrow 1}}{r_{mw} + \bar{\nu}_{2 \rightarrow 1}}. \quad (22)$$

According to this equation the $1/B$ -periodic dependence of the decay rate $\bar{\nu}_{2 \rightarrow 1}$ with sharp maxima in the vicinity of the level-matching points B_{m^*} induces a $1/B$ -periodic dependence of the fractional occupancies \bar{n}_2 and \bar{n}_1 .

In experiments^{7,8}, the half-width of the MW resonance was limited by the inhomogeneous broadening ($\gamma_{mw}/\pi \simeq 0.3 \text{ GHz}$). We shall use this estimate in the following numerical evaluations. For typical $\Omega_R/2\pi \simeq 15.9 \text{ MHz}$, the results of calculation of \bar{n}_2 are presented in Fig. 2. Variations of \bar{n}_2 are shown in the vicinity of the level-matching point B_4 vs the parameter $\omega_{2,1}/\omega_c - 4$. Far away from the level-matching point, $\bar{\nu}_{2 \rightarrow 1}$ is nearly zero and, therefore, $\bar{n}_2 \rightarrow \bar{n}_1 \rightarrow 1/2$. In the vicinity of B_4 , the occupancy \bar{n}_2 drops according to the sharp increase in the decay rate. The inelastic effect broadens the \bar{n}_2 minima, and leads to small local maxima at the level-matching points. The local peak at $\omega_{2,1}/\omega_c = 4$ becomes more pronounced with cooling, as shown in this figure by

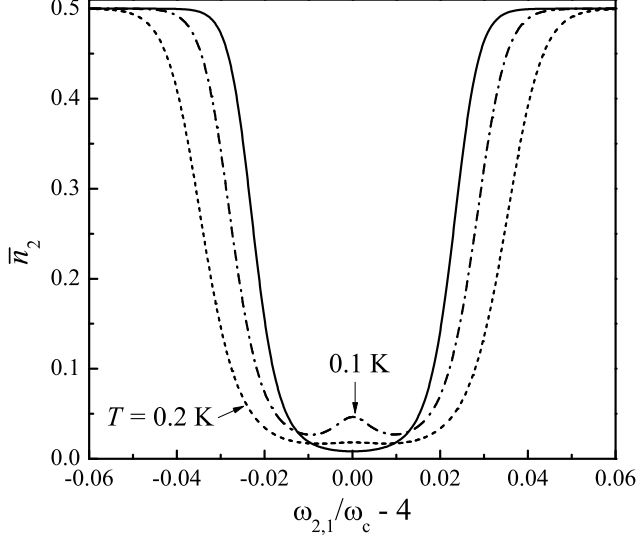


FIG. 2. The occupancy of the first excited subband vs $\omega_{2,1}/\omega_c - 4$ for $n_e = 1 \cdot 10^{16} \text{ cm}^{-2}$: elastic treatment at $T = 0.2 \text{ K}$ (solid), inelastic theory for $T = 0.2 \text{ K}$ (dashed) and $T = 0.1 \text{ K}$ (dash-dotted).

the dash-dotted line.

For SEs on liquid helium at $E_\perp = 0$, there is a spectrum crowding: $\Delta_l \rightarrow 0$ at $l \rightarrow \infty$. Therefore, at low holding fields, there is a good chance to meet the MW resonance condition for three surface subbands simultaneously: $\omega = \omega_{2,1} = \omega_{k,2}$ where k is substantially larger than 2. In wide ranges between the level-matching points B_{m^*} introduced above for the first excited subband, the decay rate $\bar{\nu}_{2 \rightarrow 1}$ is very small, and the occupancy of the third subband \bar{n}_k can also satisfy the condition $\bar{n}_k - e^{-\Delta_{k,1}/T_e} \bar{n}_1 > 0$ necessary for the appearance of the sign-changing correction to σ_{xx} . Since $\omega_{k,1} = 2\omega_{2,1}$, the new level-matching condition $\omega_{k,1}/\omega_c = m^*$ defined for the decay from $l = k$ to $l' = 1$ can be rewritten as

$$\frac{\omega_{2,1}}{\omega_c} = m^*/2. \quad (23)$$

Thus, oscillatory features of σ_{xx} could appear also at fractional values of the ratio ω/ω_c .

D. Magnetoconductivity variations induced by the MW resonance

Using the quantities $\bar{\nu}_{l,l'}^{(+)}(\mathbf{q})$ and $\bar{\nu}_{l,l'}^{(-)}(\mathbf{q})$ the frictional force \mathbf{F}_{fric} acting on the whole electron system can be evaluated directly: at first we multiply these average probabilities by $N_e \bar{n}_l \hbar \mathbf{q}$, and then perform summation over all \mathbf{q} and the subband numbers l and l' . Since we intend to obtain the conductivity of interior electrons ignoring edge effects, consider an uniform and infinite electron layer. In this case, the kinetic friction \mathbf{F}_{fric}

is antiparallel and proportional to the current^{15,25,26}, which can be written as $\mathbf{F}_{\text{fric}} = -N_e m_e \nu_{\text{eff}} \langle \mathbf{v} \rangle$, where $\langle \mathbf{v} \rangle$ is the average electron velocity. The proportionality factor ν_{eff} represents an effective collision frequency, because balancing \mathbf{F}_{fric} and the average Lorentz force $\langle \mathbf{F}_{\text{ext}} \rangle = -N_e e \mathbf{E}_\parallel - N_e m_e \omega_c [\langle \mathbf{v} \rangle \times \hat{\mathbf{z}}]$ yields the conventional Drude form for the conductivity tensor $\sigma_{i,k}$ with ν_{eff} standing instead of the semi-classical collision frequency. It should be emphasized that here ν_{eff} is not a semi-classical quantity because it depends on B and n_e .

The simplest way to obtain ν_{eff} is to consider the component $(\mathbf{F}_{\text{fric}})_y$ and to assume that the magnetic field is strong enough ($\omega_c \gg \nu_{\text{eff}}$): $\langle v_y \rangle \simeq -V_H$. Then, we can represent ν_{eff} as

$$\nu_{\text{eff}} = \frac{1}{m_e V_H} \sum_{l,l'} \bar{n}_l \sum_{\mathbf{q}} \hbar q_y [\bar{\nu}_{l,l'}^{(+)}(\mathbf{q}) + \bar{\nu}_{l,l'}^{(-)}(\mathbf{q})]. \quad (24)$$

According to (7) and (9), the right side of this relationship is actually a nonlinear function of V_H . Therefore, one has to expand it in $q_y V_H$. From the first glance at $S_{l,l'}(\Omega)$ given in Eq. (14) one may conclude that $\hbar q_y V_H / \tilde{\Gamma}_{l,n;l',n'}$ is the main expansion parameter. Still, an accurate analysis employing the relationship of Eq. (11) indicates that for intra-subband scattering at $T_e = T$ the actual expansion parameter equals $\hbar q_y V_H / T_e$. Therefore, before proceeding with the expansion of the right side of Eq. (24) we shall transform it into the form containing $S_{l,l'}$ with positive frequency arguments only.

For intra-subband scattering $\omega_{l,l'} = 0$, the basic property of Eq. (11) applied to $S_{l,l}(q, -\omega_q + q_y V_H)$ yields

$$\begin{aligned} \nu_{\text{intra}} = & \frac{1}{m_e V_H} \sum_l \bar{n}_l \sum_{\mathbf{q}} u_{l,l}^2 \hbar q_y S_{l,l}(\omega_q + q_y V_H) \times \\ & \times \left[1 - e^{\hbar \omega_q (1/T - 1/T_e)} e^{-\hbar q_y V_H / T_e} \right]. \end{aligned} \quad (25)$$

Here we have changed the sign of the summation index \mathbf{q} in the term with $S_{l,l}(\omega_q - q_y V_H)$. At $T_e = T$ and low V_H , the expression in the square brackets is proportional to $\hbar q_y V_H / T_e$. Therefore, one can neglect $q_y V_H$ in the frequency argument of the DSF. This confirms the above given statement that for intra subband scattering $\hbar q_y V_H / T_e$ is the main expansion parameter.

In the general case ($T_e \neq T$), one has to expand the exponential function in $\hbar \omega_q (1/T - 1/T_e)$ and the DSF in $q_y V_H$ as well. This gives two terms ($\nu_{\text{intra}} = \nu_{\text{intra}}^{(0)} + \nu_{\text{intra}}^{(1)}$):

$$\nu_{\text{intra}}^{(0)} = \frac{1}{m_e T_e} \sum_l \bar{n}_l \sum_{\mathbf{q}} u_{l,l}^2 \hbar^2 q_y^2 S_{l,l}(q, \omega_q), \quad (26)$$

$$\nu_{\text{intra}}^{(1)} = -\frac{T_e - T}{m_e T T_e} \sum_l \bar{n}_l \sum_{\mathbf{q}} u_{l,l}^2 \hbar^2 q_y^2 \omega_q S'_{l,l}(q, \omega_q). \quad (27)$$

Here and below $S'_{l,l'} = \partial S_{l,l'}/\partial\omega$. The term $\nu_{\text{intra}}^{(0)}$ coincides with the well-known result obtained previously for intra-subband scattering¹⁵. In the limit $n_e \rightarrow 0$, it transforms into the result of the conventional SCBA theory¹⁸. The second term appears only for $T_e \neq T$ when the scattering is substantially inelastic. Therefore, it is not an equilibrium property of the system. In the absence of the MW field, it can appear only as a nonlinear correction.

Consider now the contribution from inter-subband scattering. In Eq. (24), one can transform terms with negative Ω ($l < l'$) into the forms with positive Ω using Eqs. (12) and (13). Thus, we have

$$\begin{aligned} \nu_{\text{inter}} = & \frac{\hbar}{m_e V_H} \sum_{l>l'} \sum_{\mathbf{q}} q_y \times \\ & \{ [\bar{n}_l - \bar{n}_{l'} e^{-\Delta_{l,l'}/T_e} e^{\hbar\omega_q(1/T_e-1/T)} e^{-\hbar q_y V_H/T_e}] \bar{\nu}_{l,l'}^{(+)}(\mathbf{q}) + \\ & + [\bar{n}_l - \bar{n}_{l'} e^{-\Delta_{l,l'}/T_e} e^{\hbar\omega_q(1/T-1/T_e)} e^{-\hbar q_y V_H/T_e}] \bar{\nu}_{l,l'}^{(-)}(\mathbf{q}) \}. \end{aligned} \quad (28)$$

The sign “-” of the second term in the square brackets appears because of the change of the summation index $\mathbf{q} \rightarrow -\mathbf{q}$ for terms containing $\bar{\nu}_{l,l'}^{(+)}(-\mathbf{q})$ and $\bar{\nu}_{l,l'}^{(-)}(-\mathbf{q})$. Expanding this equation in $q_y V_H$ we find that linear in V_H terms of the square brackets yield a positive (normal) contribution

$$\begin{aligned} \nu_{\text{inter}}^{(N)} = & \frac{\hbar^2}{m_e T_e} \sum_{l>l'} \bar{n}_{l'} e^{-\Delta_{l,l'}/T_e} \sum_{\mathbf{q}} u_{l,l'}^2 q_y^2 \times \\ & \times \{ S_{l,l'}(\omega_{l,l'} - \omega_q) + S_{l,l'}(\omega_{l,l'} + \omega_q) \}. \end{aligned} \quad (29)$$

Here we used the condition $\hbar\omega_q \ll T$. If the electron system is not heated high ($T_e \ll \Delta_{l,l'}$), this contribution is exponentially small.

Under MW excitation, the major contribution to ν_{inter} comes from the expansion of the DSF entering $\bar{\nu}_{l,l'}^{(+)}(\mathbf{q})$ and $\bar{\nu}_{l,l'}^{(-)}(\mathbf{q})$:

$$\begin{aligned} \nu_{\text{inter}}^{(A)} = & \frac{1}{m_e} \sum_{l>l'} \sum_{\mathbf{q}} \hbar q_y^2 u_{l,l'}^2 \times \\ & \{ [\bar{n}_l - \bar{n}_{l'} e^{-\Delta_{l,l'}/T_e} e^{\hbar\omega_q(1/T_e-1/T)}] \times \\ & \times e^{\hbar\omega_q/T} S'_{l,l'}(\omega_{l,l'} - \omega_q) + \\ & + [\bar{n}_l - \bar{n}_{l'} e^{-\Delta_{l,l'}/T_e} e^{\hbar\omega_q(1/T-1/T_e)}] S'_{l,l'}(\omega_{l,l'} + \omega_q) \}. \end{aligned} \quad (30)$$

These anomalous terms are proportional to the derivative of $S_{l,l'}(\Omega)$. The Eq. (30) can be simplified considering

the two-subband model with $T_e = T$ and $\hbar\omega_q/T \ll 1$. Then, we obtain

$$\begin{aligned} \nu_{\text{inter}}^{(A)} = & \frac{\hbar}{m_e} (\bar{n}_2 - \bar{n}_1 e^{-\Delta_{2,1}/T_e}) \times \\ & \times \sum_{\mathbf{q}} u_{2,1}^2 q_y^2 [S'_{2,1}(\omega_{2,1} - \omega_q) + S'_{2,1}(\omega_{2,1} + \omega_q)]. \end{aligned} \quad (31)$$

From this equation, one can see that the anomalous contribution $\nu_{\text{inter}}^{(A)}$ is proportional to $\bar{n}_2 - \bar{n}_1 e^{-\Delta_{2,1}/T_e}$ and to the sign-changing terms $(\omega_{2,1} \pm \omega_q - m\omega_c)$, as expected from the qualitative analysis given in the Introduction.

In the elastic theory, $\nu_{\text{inter}}^{(A)}$ changes its sign once in the vicinity of each B_{m*} . When the inelastic effect is substantial, the expression in the square brackets is a derivative of the function which has two maxima and one minima near each B_{m*} . Therefore, in the vicinity of a level-matching point, the anomalous contribution caused by inelastic inter-subband scattering changes its sign three times.

It should be noted that here we use slightly different definitions of the normal $\nu_{\text{inter}}^{(N)}$ and anomalous $\nu_{\text{inter}}^{(A)}$ contributions than that given before^{12,17}. Now we apply labels N and A to the corresponding expressions which are transformed into the form containing the summation over $l > l'$ only. For such definition, $\nu_{\text{inter}}^{(N)}$ becomes substantially smaller, and $\nu_{\text{inter}}^{(A)}$ does not contain small terms which are not proportional to $S'_{2,1}(\Omega)$ with $\Omega > 0$. In the limiting case $\hbar\omega_q \rightarrow 0$, the sum of $\nu_{\text{inter}}^{(A)}$ and $\nu_{\text{inter}}^{(N)}$ obviously coincides with that found previously in the elastic treatment.

III. RESULTS AND DISCUSSION

In the following evaluations, we shall consider strictly the approximation $T_e \simeq T$ and fix $\omega_{2,1}/2\pi$ to 140 GHz which corresponds to $E_{\perp} = 28$ V/cm for SEs on liquid ⁴He. The situation when T_e differs substantially from T will be analyzed only qualitatively. At typical temperatures of the ripplon scattering regime $T \leq 0.3$ K, we can restrict ourselves to the ultra-quantum limiting case ($\hbar\omega_c \gg T_e$). Then, Eq. (26) can be represented as

$$\begin{aligned} \nu_{\text{intra}}^{(0)} = & \frac{\omega_c T}{4\sqrt{\pi}\alpha T_e} \sum_l \bar{n}_l \times \\ & \times \int_0^\infty \frac{|(U_q)_{l,l}|^2}{\tilde{\Gamma}_{l,0;l,0}^2} \exp\left[-x_q - \frac{(\hbar\omega_q)^2}{\tilde{\Gamma}_{l,0;l,0}^2}\right] dx_q, \end{aligned} \quad (32)$$

This equations shows how the inelastic effect suppresses the contribution from intra-subband scattering. Magneto-oscillations of $\nu_{\text{intra}}^{(0)}$ are due to variations of $\bar{n}_l(B)$ discussed above and $T_e(B)$ if electron heating

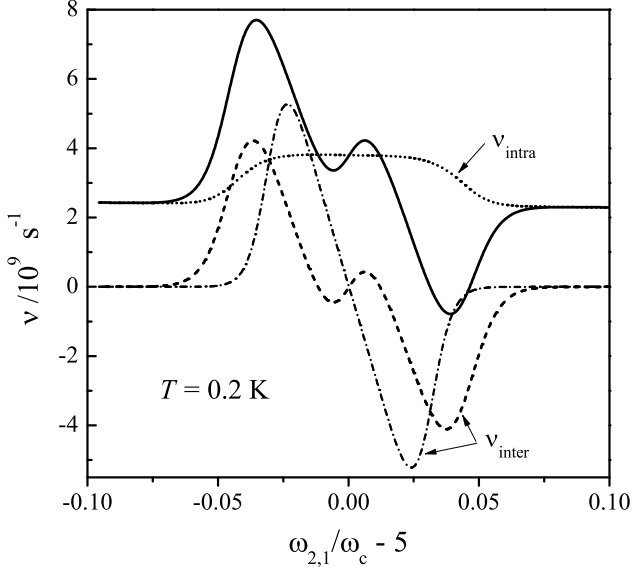


FIG. 3. Different contributions into the effective collision frequency near the level-matching point B_5 vs the parameter $\omega_{2,1}/\omega_c - 5$ for $T_e = T = 0.2$ K and $n_e = 1 \cdot 10^6 \text{ cm}^{-2}$: inelastic treatment for intra-subband scattering (dotted), inter-subband scattering for elastic (dash-dotted) and inelastic (dashed) theories. The total collision frequency is shown by the solid line.

becomes important. For $T_e = T$, the typical shape of these oscillations is shown in Fig. 3 by the dotted line. These evaluations have employed the $n_l(B)$ of the two-subband model. We do not show the corresponding line calculated for the elastic approximation because it has a similar shape: just a narrower and higher maximum.

In the same way, the nonequilibrium correction $\nu_{\text{intra}}^{(1)}$ can be found as

$$\nu_{\text{intra}}^{(1)} = \frac{T_e - T}{T_e} \frac{\omega_c}{2\sqrt{\pi}\alpha} \sum_l \bar{n}_l \times \int_0^\infty \frac{|(U_q)_{l,l'}|^2}{\tilde{\Gamma}_{l,0;l,0}^2} \frac{(\hbar\omega_q)^2}{\tilde{\Gamma}_{l,0;l,0}^2} \exp\left\{-x_q - \frac{(\hbar\omega_q)^2}{\tilde{\Gamma}_{l,0;l,0}^2}\right\} dx_q. \quad (33)$$

This contribution becomes important when T_e substantially exceeds T . As compared to Eq. (32), its integrand contains an additional parameter $(\hbar\omega_q/\tilde{\Gamma}_{l,0;l,0})^2$.

According to Eq. (32) with an increase in T_e the contribution $\nu_{\text{intra}}^{(0)}$ decreases as $1/T_e$ if the Coulomb broadening Γ_C can be neglected. For a finite electron density, the Coulombic effect eventually changes this dependence into $1/T_e^{3/2}$. On the contrary, $\nu_{\text{intra}}^{(1)}$ increases first with T_e approaching a saturation. Then, the Coulombic effect leads to a decrease with the similar dependence $1/T_e^{3/2}$. Magneto-oscillations of $\nu_{\text{intra}}^{(1)}$ crucially depend on electron temperature oscillations. Still, the calculation of

$T_e(B)$ requires the knowledge of the electron energy relaxation rate which will not be discussed in the present work.

As noted above, the contribution $\nu_{\text{inter}}^{(N)}$ is exponentially small, and it can be neglected in calculations with $T_e \simeq T$. In the ultra-quantum limit, the contribution $\nu_{\text{inter}}^{(A)}$ can be transformed into

$$\begin{aligned} \nu_{\text{inter}}^{(A)} = & -\frac{\omega_c T}{2\sqrt{\pi}\alpha} \sum_{l>l'} \left(\bar{n}_l - \bar{n}_{l'} e^{-\Delta_{l,l'}/T_e} \right) \times \\ & \times \sum_{m=0}^{\infty} \frac{1}{m!} \int_0^\infty dx_q \frac{|(U_q)_{l,l'}|^2}{\tilde{\Gamma}_{l,0;l',m}^2} x_q^m e^{-x_q} \times \\ & \times \left[R_{l,l',m}^{(+)}(x_q) I_{l,l',m}^{(+)}(x_q) + R_{l,l',m}^{(-)}(x_q) I_{l,l',m}^{(-)}(x_q) \right]. \end{aligned} \quad (34)$$

This equation shows the way how the inelastic effect affects magneto-oscillations of ν_{inter} . Firstly, we note that the integrand of Eq. (34) contains the factor $x_q^m e^{-x_q}$ which enhances the inelastic effect ($\omega_q \propto x_q^{3/4}$) in the low field range where the level-matching numbers m^* are larger. It enhances also the Coulombic correction to the broadening parameter $\tilde{\Gamma}_{l,0;l',m}$. Therefore, to observe the inelastic effect on magneto-oscillations of σ_{xx} electron densities must be sufficiently low.

The results of numerical evaluations of $\nu_{\text{inter}}^{(A)}$ are given in Fig. 3 for $B \approx B_5$. Variations of $\nu_{\text{inter}}^{(A)}$ obtained in the elastic approximation are shown by the dash-dotted line. It changes sign only once. The dashed line calculated according to the inelastic theory changes its sign three times. Remarkably, at $B = B_5$ the slope of this line is changed to the opposite, as compared to the result of the elastic theory. Thus, we have a fine oscillatory structure in the vicinity of the level-matching point caused by the inelastic effect. The total collision frequency ν_{eff} is shown by the solid line. For the chosen excitation rate, ν_{eff} acquires negative values which leads to negative conductivity effects. The condition $\sigma_{xx} < 0$ was previously shown²⁷ to be the origin of zero-resistance states.

The evolution of the shape of magnetoconductivity variations near B_{m^*} is illustrated in Fig. 4 for $m^* = 1, 2, \dots, 7$ and $T_e = T$. The inelastic effect displays itself as an additional wavy variation in the vicinity of $\omega_{2,1}/\omega_c - m^* = 0$. For $m^* = 1$, the inelastic effect is not strong and the corresponding line just shows an additional plateau at the level-matching condition. The inelastic effect becomes stronger for larger m^* (lower magnetic fields): the amplitude of new wavy variations of σ_{xx} increases. Then, at $m^* = 5$ the amplitude of variations caused by the inelastic effect starts to decrease, and at $m^* = 6$ a new plateau appears at the level-matching point. This reduction of the inelastic effect is caused by the corresponding increase in the Coulomb broadening of the generalized DSF.

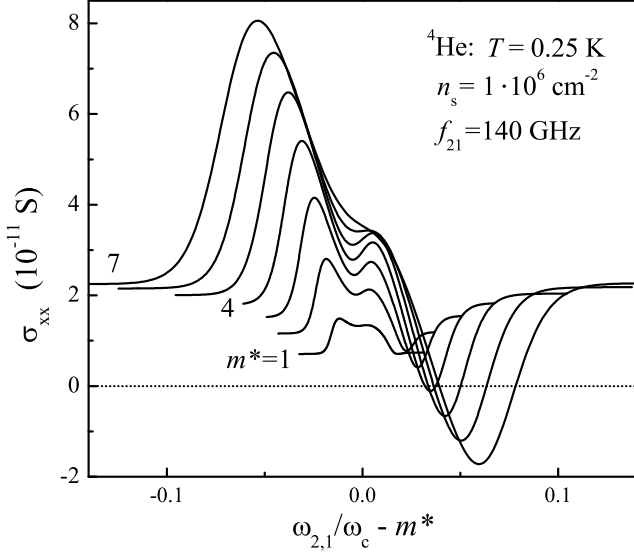


FIG. 4. Magnetoconductivity near the level-matching points B_{m^*} vs $\omega_{2,1}/\omega_c - m^*$ for $m^* = 1, 2, 3, \dots, 7$.

The broadening of the DSF decreases with cooling $\tilde{\Gamma}_{l,0;l',m} \propto \sqrt{T}$ if the holding field is low. Therefore, the inelastic effect becomes more pronounced at lower temperatures. This is illustrated in Fig. 5 where σ_{xx} is plotted vs B in the vicinity of $B_5 = 1$ T for three different temperatures. At $T = 0.3$ K the inelastic effect displays itself as a plateau feature appeared at $B = B_5$. At lower T it transforms into a wavy line whose amplitude increases sharply with cooling.

The Coulomb broadening of the DSF $\sqrt{x_q}\Gamma_C$ increases strongly with electron density. Therefore, with a substantial increase in n_e the inelastic effect becomes suppressed, as illustrated in Fig. 6. This figure shows the shape of magnetoconductivity oscillations near $B_4 = 1.25$ T for three different electron densities. One can see that the increase of n_e by the factor 3 eliminates the fine wavy structure introduced by inelastic scattering. The Fig. 6 can be used also for modeling of the influence of electron heating on the inelastic effect. Since $\Gamma_C \propto T_e^{1/2} n_e^{3/4}$, the increase of T_e by the factor $3^{3/2}$ produces the same Coulomb broadening and the same reduction of the inelastic effect as the increase of n_e by the factor 3 which is shown in the figure. It should be noted also that electron heating can affect the height of the new wavy anomaly by the decrease of ν_{intra} discussed above.

Holding electric field E_{\perp} increases the frequency $\omega_{2,1}$ and the characteristic magnetic fields B_{m^*} which favours the inelastic effect. On the other hand, a larger E_{\perp} increases the collision broadening of Landau levels which reduces the inelastic parameter $\hbar\omega_q/\Gamma_{l,n}$. Therefore, the holding field should be kept much smaller than the effective field of the image potential contributing into the

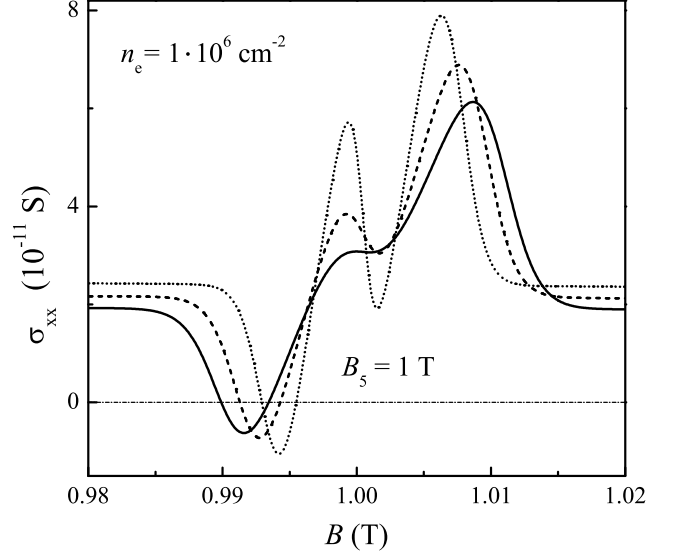


FIG. 5. Magnetoconductivity vs B near the level-matching point B_5 for different temperatures: 0.3 K (solid), 0.2 K (dashed), and 0.1 K (dotted).

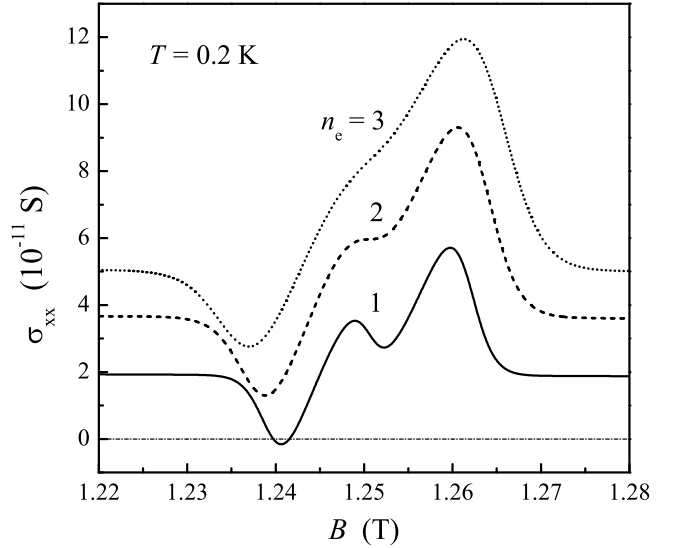


FIG. 6. Magnetoconductivity vs B near the level-matching point $B_4 = 1.25$ T for three different electron densities n_e shown in units of 10^6 cm^{-2} .

electron-ripplon coupling: $E_{\perp}^{(\text{eff})} \sim 180 \text{ V/cm}$ at $B \sim 1$ T. At the same time, in the limit of low holding fields, there is a chance to meet the resonance condition for three surface subbands simultaneously, as noted in the previous Section. In this case, the shape of magnetoconductivity oscillations will be affected by an additional filling of the third resonant subband $\bar{n}_k > \bar{n}_1 e^{-\Delta_{k,1}/T_e}$, and there

might be additional variations of σ_{xx} at fractional values of the ratio ω/ω_c caused by electron scattering from the third subband ($l = k$) to the ground subband ($l = 1$). The results of these evaluations will be given elsewhere.

IV. CONCLUSIONS

We have presented theoretical description of MW-resonance-induced magnetoconductivity oscillations for surface electrons on liquid helium under the condition that the energy exchange at a collision cannot be neglected as compared to the Landau level broadening. Such a condition can be realized for SEs on liquid ^4He at low temperatures ($T \leq 0.2\text{K}$) and weak holding fields. The inelastic effect discussed here is shown to affect differently the decay rate of the excited subband and the electron momentum relaxation rate caused by inter-subband scattering. Near the level matching points ($B \simeq B_{m^*}$) the decay maxima are split because of ripplon destruction and creation processes. This splitting surprisingly becomes stronger in the low magnetic field range

because of the enhancement factor $m^* = \text{round}(\omega_{2,1}/\omega_c)$. At the same time, magnetoconductivity variations induced by the inelastic effect represent a mixture of splitting and inversion. As a result, a new wavy feature can be realized on the shape of magnetoconductivity oscillations in the vicinity of the level-matching points. The amplitude of this fine structure increases in the range of low magnetic fields, which is contrary to the inelastic effect observed for intra-subband scattering¹⁴.

We have studied the influence of strong electron-electron interaction and possible heating of the electron system on the display of the inelastic effect in photoconductivity oscillations. The results obtained indicate that a substantial increase in electron density n_e above $1 \cdot 10^6 \text{cm}^{-2}$ reduces strongly new wavy variations of $\sigma_{xx}(B)$ induced by the inelastic effect. Similar reduction in the display of the inelastic effect is expected if the electron system is heated strongly because of the decay of excited subbands. Fortunately, the negative effect of electron heating is caused by the Coulomb broadening of the generalized dynamic structure factor of the multi-subband 2D electron system which can be reduced by a proper decrease in electron density.

-
- ¹ M.A. Zudov, R.R. Du, J.A. Simmons, and J.R. Reno, Phys. Rev. B **64**, 201311(R) (2001).
 - ² R. Mani, J.H. Smet, K. von Klitzing, V. Narayanamurti, W.B. Johnson, and V. Umansky, Nature **420**, 646 (2002).
 - ³ M.A. Zudov, R.R. Du, L.N. Pfeiffer, and K.W. West, Phys. Rev. Lett. **90**, 046807 (2003).
 - ⁴ A.C. Durst, S. Sachdev, N. Read, and S.M. Girvin, Phys. Rev. Lett. **91**, 086803 (2003).
 - ⁵ I.A. Dmitriev, M.G. Vavilov, I.L. Aleiner, A.D. Mirlin, and D.G. Polyakov, Phys. Rev. B **71**, 115316 (2005).
 - ⁶ S.A. Mikhailov, Phys. Rev. B **83**, 155303 (2011).
 - ⁷ D. Konstantinov and K. Kono, Phys. Rev. Lett. **103**, 266808 (2009).
 - ⁸ D. Konstantinov and K. Kono, Phys. Rev. Lett. **105**, 226801 (2010).
 - ⁹ M.W. Cole and M.H. Cohen, Phys. Rev. Lett. **23**, 1238 (1969).
 - ¹⁰ V.B. Shikin, Soviet Phys. JETP **31**, 936. (1970) [Zh. Eksperim. teor. Fiz. **58**, 1748 (1970)].
 - ¹¹ Yu.P. Monarkha, Fiz. Nizk. Temp. **37**, 108 (2011) [Low Temp. Phys. **37**, 90 (2011)].
 - ¹² Yu.P. Monarkha, Fiz. Nizk. Temp. **37**, 829 (2011) [Low Temp. Phys. **37**, 655 (2011)].
 - ¹³ V. I. Ryzhii, Fiz. Tverd. Tela **11**, 2577 (1969) [Sov. Phys. Solid State **11**, 2078 (1970)]; V.I. Ryzhii, R.A. Suris, and B. S. Shchamkhalova, Fiz. Tekh. Poluprovodn. **20**, 2078 (1986) [Sov. Phys. Semicond. **20**, 1299 (1986)].
 - ¹⁴ Yu.P. Monarkha, S. Ito, K. Shirahama, and K. Kono, Phys. Rev. Lett. **78**, 2445 (1997).
 - ¹⁵ Yu.P. Monarkha and K. Kono, *Two-Dimensional Coulomb Liquids and Solids*, Springer-Verlag, Berlin Heidelberg (2004).
 - ¹⁶ D. Konstantinov, Chepelianskii, and K. Kono, J. Phys. Soc. Jpn. **81**, 093601 (2012).
 - ¹⁷ Yu.P. Monarkha, Low Temp. Phys. **38**, 451 (2012) [Fiz. Nizk. Temp. **38**, 579 (2012)].
 - ¹⁸ T. Ando and Y. Uemura, J. Phys. Soc. Jpn. **36**, 959 (1974).
 - ¹⁹ R. Kubo, S.J. Miyake, N. Hashitsume, Solid State Phys. **17**, 269 (1965).
 - ²⁰ Yu.P. Monarkha, S.S. Sokolov, A.V. Smorodin, and N. Stuard, Low Temp. Phys. **36**, 565 (2010) [Fiz. Nizk. Temp., **36**, 711 (2010)].
 - ²¹ W. Marshall and S.W. Lovesey: *Theory of Thermal Neutron Scattering* (Clarendon Press, Oxford 1971).
 - ²² R.R. Gerhardts, Surf. Sci. **58**, 227 (1976).
 - ²³ M.I. Dykman and L.S. Khazan, Sov. Phys. JETP **50**, 747 (1979) [Zh. Eksp. Teor. Fiz. **77**, 1488 (1979)].
 - ²⁴ D. Konstantinov, H. Isshiki, Yu. Monarkha, H. Akimoto, K. Shirahama, and K. Kono, Phys. Rev. Lett. **98**, 235302 (2007).
 - ²⁵ P.J.M. Peters, P. Scheuzger, M.J. Lea, Yu.P. Monarkha, P.K.H. Sommerfeld, and R.W. van der Heijden, Phys. Rev. B **50**, 11570 (1994).
 - ²⁶ Yu.P. Monarkha, E. Teske, and P. Wyder, Phys. Rep. **370**, No. 1, pp. 1-61 (2002).
 - ²⁷ A.V. Andreev, I.L. Aleiner, and A.J. Millis, Phys. Rev. Lett., **91**, 056803 (2003).